Age-hardening behaviors and grain boundary discontinuous precipitation in a Pd-free gold alloy for porcelain bonding

TAKANOBU SHIRAISHI*
Department of Dental Materials Science, Nagasaki University School of Dentistry, Nagasaki 852-8588, Japan
E-mail: siraisi@net.nagasaki-u.ac.jp

MICHIO OHTA
Section of Biomaterials Engineering, Faculty of Dental Science, Kyushu University, Fukuoka 812-8582, Japan

Isothermal age-hardening behaviors at 400° and 450 °C and discontinuous precipitation reaction at 450 °C in a commercial Pd-free gold alloy for porcelain bonding were investigated by hardness testing, X-ray powder diffraction, and light microscopy. Variations of electrical resistivity during continuous heating and cooling processes were also measured. The alloy exhibited pronounced age-hardening in the early stage of aging and the maximum hardness exceeded twice that of the solution-treated sample. Precise lattice parameter measurements and investigations of full width at half maximum values for the X-ray Bragg reflections implied that nonuniform strains due to the pre-precipitation or zone formation was responsible for the quick and pronounced age-hardening at 450 °C. Discontinuous precipitation reaction, producing a mixture of a small amount of Pt_3In-phase with the $L1_2$-type superstructure and a large amount of (Pt, In)-depleted solid solution, started at grain boundaries in the late stage of aging process at 450 °C. The growth of the grain boundary discontinuous precipitates toward the intragrain area led to a gradual decrease in hardness of the alloy.

1. Introduction

Dental porcelain-fused-to-metal restorations possess both excellent biocompatibility and aesthetics of porcelain and distinguished toughness of metallic frames. Various types of compositions have been developed since the introduction of porcelain-fused-to-metal restorations in dentistry. Among them high-karat gold alloys, basically composed of gold, platinum, palladium, and a small quantity of others, have been served for long periods.

Recently, newly developed Pd-free high-karat gold alloys for porcelain bonding were introduced into the market primarily to serve as an attractive material for some patients who are allergic or hypersensitive to palladium. Recent clear trend of the growing emphasis in biocompatibility and aesthetics of dental restorative materials and rising price of palladium [1] may promise the increasing use of this new type of Pd-free gold alloys for porcelain bonding.

It is essential that the metallic frames of porcelain-fused-to-metal restorations possess high mechanical strength to prevent the peeling or fracture of the porcelain. In fact, isothermal age-hardening treatment after the porcelain firing process is sometimes directed by the manufacturers to improve the strength of the metallic frame. Although phase transformations in several traditional gold alloys for porcelain bonding have been investigated [2–5], phase transformation and age-hardening behaviors of the Pd-free gold alloys for porcelain bonding have not been clarified.

The objectives of this study were to investigate age-hardening behaviors at 400° and 450 °C and to clarify phase transformation in a new commercial Pd-free high-karat gold alloy for porcelain bonding.

2. Material and methods

2.1. Material

Nominal composition in mass percentage of the alloy examined is listed in Table I. This alloy is composed mainly of gold and platinum with small additions of indium, rhodium, zinc, and tantalum.

2.2. Electrical resistivity measurements

A sheet sample of size $2 \times 20 \times 0.15\,mm^3$ was solution-treated at 950 °C for 30 min in high-purity argon gas

*Author to whom all correspondence should be addressed.

TABLE I Nominal composition of the alloy examined (mass %)

Alloy	Manufacturer	Lot number	Au	Pt	In	Rh	Zn	Ta
BiOcclus 4	Degussa AG (Germany)	G012188	85.8	11.0	1.7	0.7	0.5	0.3

stream and quenched into ice-brine. A couple of nickel wires of 0.3 mm in diameter were spot-welded to each end of this sheet sample as current-leading and potential-measuring wires. Then the sample with nickel wires was placed in an evacuated silica glass tube and continuously heated up to 950 °C at a constant rate of 0.5 °C/min and subsequently cooled down to room temperature at the same rate. Changes in electrical resistivity during this thermal excursion were measured with the four-terminal potentiometric method with a direct current of 200 mA.

2.3. Hardness testing

A plate sample of size $3 \times 10 \times 0.8\,mm^3$ was subjected to the above-described solution treatment and subsequently aged in a salt bath regulated at 400° or 450 °C for various periods. Hardness testing was carried out on these samples using a Vickers microhardness tester (MXT 50, Matsuzawa Seiki Co., Ltd., Tokyo, Japan) with a load of 300 gf and a dwell time of 10 s. The mean hardness number and standard deviation were obtained from five indentations.

2.4. X-ray powder diffraction

Powder samples that passed through a 330-mesh screen were prepared using a rotating diamond disk. The powders obtained were sealed in an evacuated silica glass capsule and subjected to the above-described solution treatment and the aging treatment at 450 °C. X-ray diffraction study was carried out on these powder samples using a standard-type diffractometer (RINT 2500V, Rigaku Denki Co. Ltd., Tokyo, Japan) equipped with a diffracted-beam monochromator. The X-ray source was a rotating-anode copper target operating at the accelerating voltage of 50 kV and the tube current of 200 mA. To detect very weak superlattice reflections from a small amount of an ordered phase, a fixed time method with the fixed time of 5 s and the increment of 0.005°(2θ) was employed.

2.5. Light microscopy

Plate samples of the same size as for the hardness testing were isothermally aged at 450 °C for desired periods and embedded into epoxy resin. They were mechanically ground using a 1500-grit SiC water-proof paper abrasive and polished using Al_2O_3 slurries. The samples were then subjected to the electrolytic lap-polishing followed by the electrolytic etching in a standard-type electro-polishing apparatus (Relapol, Struers Scientific Instruments, Copenhagen, Denmark). Microstructures of these samples were observed using a light microscope (PME-1, Olympus Optical Co., Ltd., Tokyo, Japan) under a bright-field illumination.

3. Results

3.1. Electrical resistivity change

Fig. 1 shows variations of electrical resistivity of the solution-treated sample during continuous heating up to 950 °C and the subsequent cooling processes at a constant rate of 0.5 °C/min. Electrical resistivity of the sample at any given temperature was expressed as normalized value by setting the resistivity value at 950 °C to unity. In the heating process, resistivity at first increased almost linearly up to about 280 °C and then began to deviate upward from the baseline as shown in the figure. After attaining the peak at about 410 °C, the resistivity considerably decreased and reached the bottom at about 580 °C and then increased again with temperature. The considerable decrease in resistivity also occurred in the cooling process. These drops of electrical resistivity suggest that some precipitation reaction occurs in this alloy. Actually, inflection points in the resistivity-temperature curves were observed at about 900 °C in the heating process and at about 880 °C in the cooling process, as indicated by double arrows in the figure. It is considered, therefore, that phase transformation temperature exists between these inflection point temperatures.

3.2. Age-hardening and overaging behaviors

Age-hardening curves for the alloy quenched from 950 °C and subsequently aged at 400 or 450 °C are shown in Fig. 2. Pronounced age-hardening occurred at both temperatures, and the maximum hardness exceeded twice that of the solution-treated samples. Age-hardening rate at 450 °C was very fast and the maximum hardness was attained within about 10 min. At both temperatures high hardness values were retained for long periods. It is shown that prolonged aging treatment at 450 °C caused the gradual decrease in hardness. The cause of this

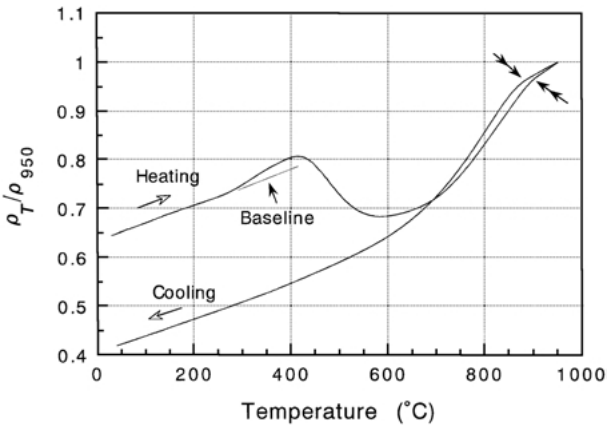

Figure 1 Changes in electrical resistivity of the quenched sample during continuous heating and the subsequent cooling processes at a constant rate of 0.5 °C/min.

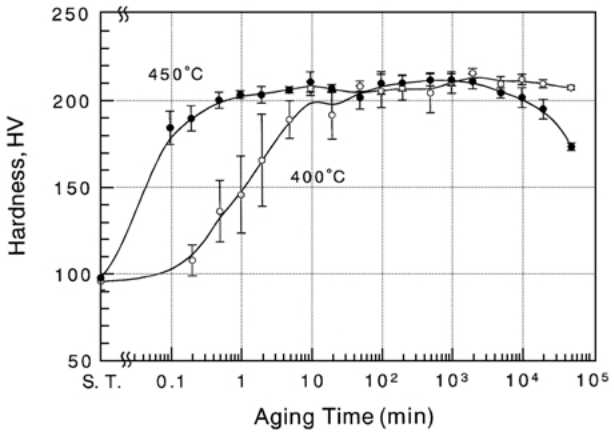

Figure 2 Age-hardening curves for the alloy aged at 400 and 450 °C. Error bars indicate standard deviations.

hardness fall in the late stage of aging will be discussed later.

3.3. X-ray diffraction

Fig. 3(a) and (b) show variations with aging time of X-ray diffraction pattern of the powder sample quenched from 950 °C and subsequently aged at 450 °C. Under the solution-treated condition, very strong and sharp reflections from a parent α'-phase with the face-centered cubic structure (FCC) were observed. Lattice parameter of the α'-phase was estimated to be $a = 0.40625$ nm. No apparent change in the diffraction pattern was observed up to the aging time of 100 min. After the passage of 1000 min, the 1 1 1 and 2 0 0 reflections from a new phase, termed β-phase tentatively, appeared at 2θ positions of about 39° and 45.3° respectively, as indicated by single arrows in Fig. 3(a). Simultaneously, the 3 3 1 and 4 2 0 reflections from a newly produced solid solution with the FCC structure, termed α-phase, appeared at 2θ positions of about 111° and 115.4° respectively, as indicated by double arrows in Fig. 3(b). Intensities of these newly appeared reflections from the α- and β-phases apparently increased with time, while those of a parent α'-phase gradually decreased and almost disappeared after the aging time of 100 000 min. It should be noted that peak positions of the parent α'-phase and the reaction products, α- and β-phases, did not change during phase transformation process. This fact indicates that the phase transformation at this temperature progressed by the discontinuous precipitation mechanism. Thus, phase transformation occurring at 450 °C can be written as:

$$\alpha' \rightarrow \alpha + \beta$$

It is clear from Fig. 3(a) and (b) that volume fraction of the β-phase in the reaction products was very small compared to that of the α-phase. The phase identification of the reaction products will be performed in the discussion section.

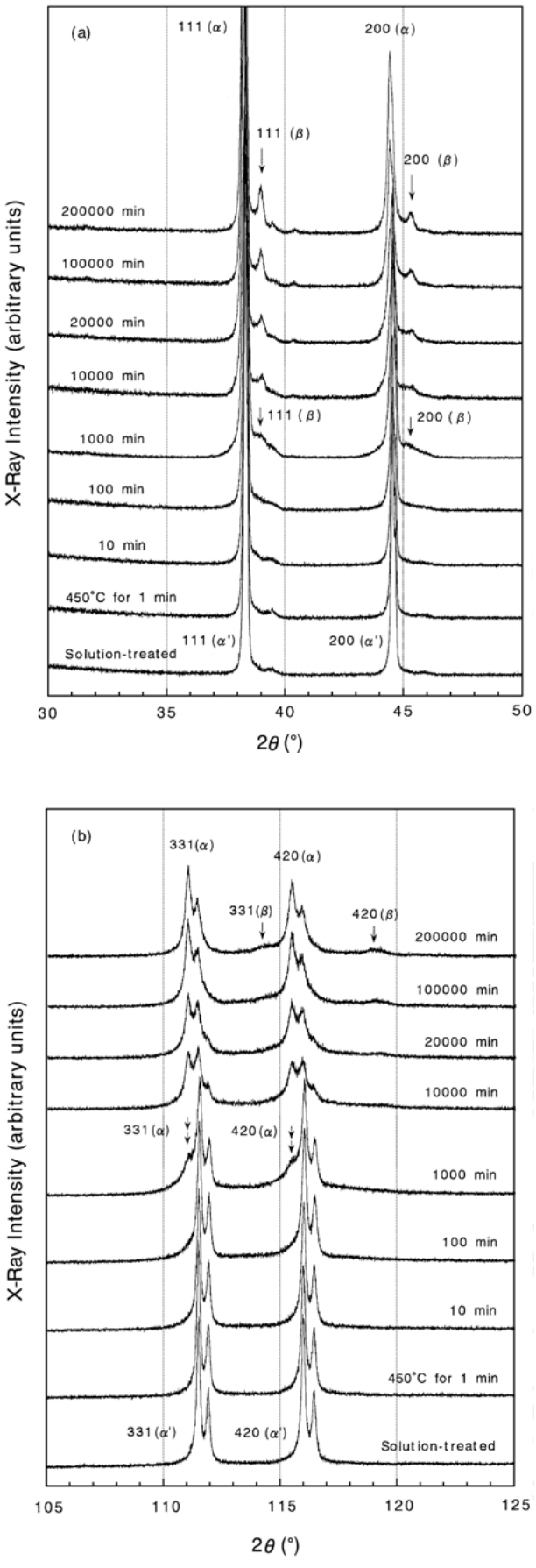

Figure 3 Variations of X-ray diffraction pattern near the 1 1 1 and 2 0 0 reflections (a) and near the 3 3 1 and 4 2 0 reflections (b) of the powder sample aged at 450 °C.

3.4. Microstructure

Fig. 4 shows a typical light micrograph of the alloy aged at 450 °C for 10 000 min, showing grain boundary discontinuous precipitates. These grain boundary precipitates appeared in the late stage of aging and slowly developed towards grain interior regions. The aging time

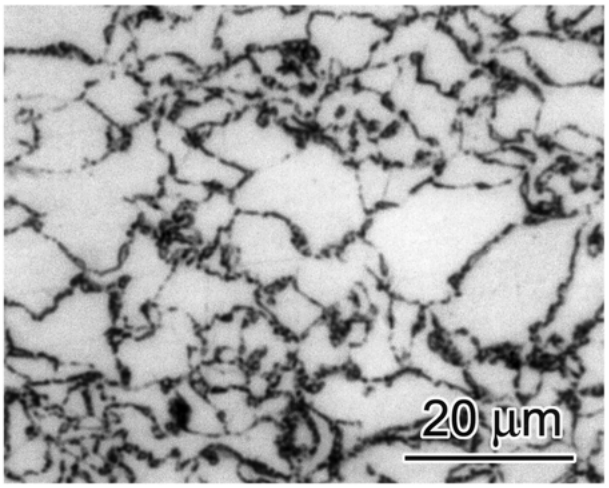

Figure 4 Light micrograph of the alloy aged at 450 °C for 10 000 min, showing grain boundary discontinuous precipitates (dark area).

at which the grain boundary precipitates appeared agrees with the aging time at which the α- and β-phases simultaneously appeared in the X-ray diffraction pattern, as shown in Fig. 3(a) and (b).

4. Discussion

4.1. Age-hardening reaction

Age-hardening at 450 °C of this alloy occurred quickly and the maximum hardness was attained at the aging time of 10 min (Fig. 2). During this age-hardening process, no apparent change in the X-ray diffraction pattern was observed, as shown in Fig. 3(a) and (b). Based on a number of examples, Krawitz and Sinclair [6] showed that precise measurements of the lattice parameter during decomposition of a supersaturated solid solution can provide a method for distinguishing pre-precipitation from precipitation in appropriate circumstances. They demonstrated that during pre-precipitation the solute atoms still diffract with the solvent atoms and the fundamental X-ray diffraction peaks are identical to those of the random supersaturated solid solution.

Thus, we investigated variations of lattice constant value of the parent α′-phase during the age-hardening process of up to 10 min at 450 °C. To evaluate lattice constant precisely, we performed precise lattice parameter measurements using many fundamental Bragg peaks [7]. To check an accuracy of lattice parameter values, we repeated precise lattice parameter measurements five times using individually-mounted same powder samples. Standard deviation of lattice constant values for such evaluation was $\pm$ 0.00001 nm, allowing detection of small changes in composition of a parent phase. Results of the precise lattice parameter measurements revealed that a lattice constant of the parent α′-phase did not change up to the aging time of 10 min at 450 °C within the experimental error. According to the above-mentioned prediction by Krawitz and Sinclair [6], present results suggest that the pre-precipitation or zone formation reaction is responsible for the quick and marked hardening at 450 °C.

Fig. 5 shows changes in full width at half maximum (FWHM) values for the principal X-ray Bragg reflections for the CuKα_1 radiation during the age-hardening process of up to 10 min at 450 °C. It is shown that the FWHM values for the Bragg reflections apparently increased with time. This indicates that nonuniform strains were introduced in the crystal lattice during this age-hardening process [8]. This finding strongly supports the above-described pre-precipitation or zone formation reaction during the age-hardening process.

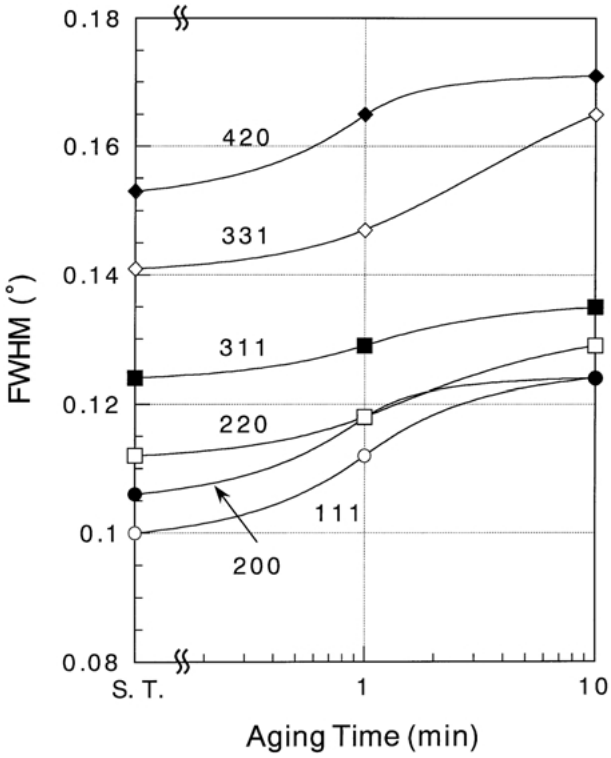

Figure 5 Variations with aging time at 450 °C of FWHM values for the principal X-ray Bragg reflections from the parent α′-phase. The FWHM values for the CuKα_1 radiation were plotted.

4.2. Discontinuous precipitation reaction

To identify the α- and β-phases in the reaction products, we first estimated their lattice parameters from the X-ray diffraction data of the powder sample aged at 450 °C for 200 000 min. They were computed to be $a = 0.40755$ nm for the α-phase and $a = 0.4003$ nm for the β-phase.

Second, we searched for superlattice reflections from the β-phase to investigate its atomic arrangement. Because the intensities of the 1 1 1 and 2 0 0 fundamental reflections from the β-phase were weak, as shown in Fig. 3(a), we employed the fixed time method to search for its very weak superlattice reflections. Fig. 6 is X-ray diffraction patterns of the powder sample aged at 450 °C for 200 000 min, showing very weak 100 (a) and 1 1 0 (b) superlattice reflections from the β-phase. The fact that both of these superlattice reflections were clearly detected indicates that the β-phase has the $L1_2$-type (Cu_3Au-type) superstructure.

The estimated lattice constant of the β-phase with the Cu_3Au-type superstructure, $a = 0.4003$ nm, is very close to the reported lattice constant, $a = 0.3992$ nm, for the binary Pt_3In-phase with the Cu_3Au-type superstructure [9]. Thus, the β-phase is considered to be the Pt_3In-phase. A possible atomic arrangement could be that of a FCC lattice with the platinum atoms located at the face-centered positions of the unit cells and indium atoms

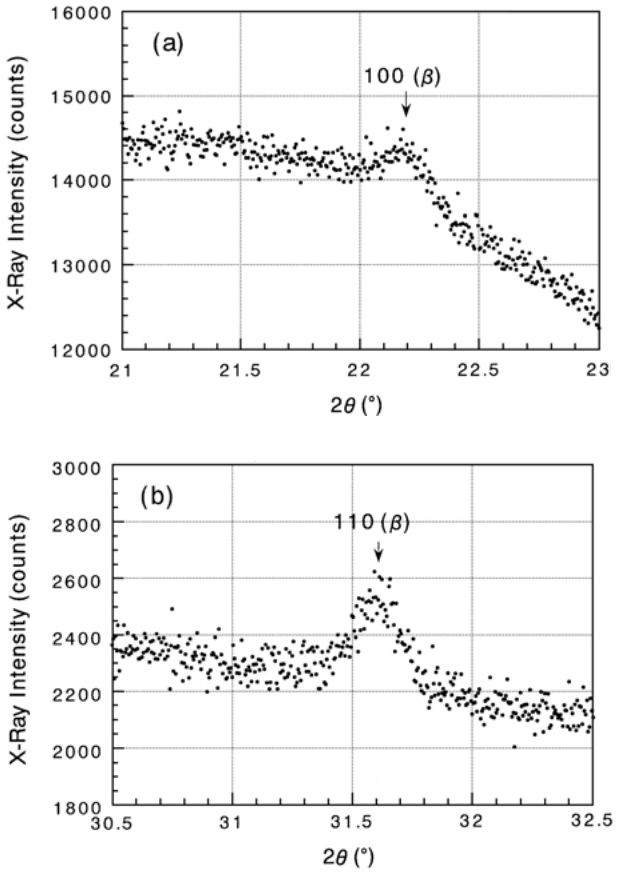

Figure 6 1 0 0 (a) and 1 1 0 (b) superlattice reflections from the β-phase with the $L1_2$-type (Cu_3Au-type) superstructure in the powder sample aged at 450 °C for 200 000 min. The fixed time method with the fixed time of 5 s at each 2θ position and an increment of 0.005° (2θ) in the X-ray diffraction technique was employed.

TABLE II Vickers hardness numbers (HV) of the grain interior region and the grain boundary precipitates in the alloy aged at 450 °C for 50 000 min (Load: 10 gf)

Region	HV
Grain interior	202.8 ± 9.7
Grain boundary precipitates	165.1 ± 3.9

occupying the corner positions. Grain boundary discontinuous precipitation occurring in the late stage of phase transformation process at 450 °C is, therefore, written as:

$$\alpha' \rightarrow \alpha + Pt_3In$$

Here, the α-phase is a (Pt, In)-depleted solid solution with the FCC structure.

Table II lists Vickers hardness numbers of the grain interior region and the grain boundary precipitates in the alloy aged at 450 °C for 50 000 min. The hardness of each region was individually measured with a light load of 10 gf. Although the grain interior region retained high hardness, the hardness of the grain boundary precipitates was considerably low. Considering the fact that the volume fraction of the grain boundary precipitates gradually increased with time, it is concluded that the growth of the grain boundary precipitates with low hardness is responsible for the overaging in the late stage of aging at 450 °C.

5. Conclusions

Isothermal age-hardening behaviors and phase transformation of a new Pd-free gold alloy for porcelain bonding were investigated mainly by hardness testing, X-ray powder diffraction, and light microscopy. Principal results obtained are as follows:

1. Nonuniform strains introduced in the crystal lattice due to the pre-precipitation or zone formation are responsible for the quick and pronounced age-hardening at 450 °C;
2. Phase transformation producing stable phases at 450 °C progresses by the grain boundary discontinuous precipitation mechanism, written as:

$$\alpha' \rightarrow \alpha + Pt_3In$$

3. The slow growth of the grain boundary discontinuous precipitates led to a gradual decrease in hardness in the overaging stage.

Acknowledgments

The authors are grateful to Drs M. Nakagawa and S. Matsuya of Faculty of Dental Science, Kyushu University and Y. Tanaka of Nagasaki University School of Dentistry for their technical assistance. One of the authors (T.S.) would like to thank Prof. K. Hisatsune of Nagasaki University School of Dentistry for his encouragement of the preparation of this paper.

References

1. ''Platinum 2000'' (Johnson Matthey, London, England, 2000) p. 8.
2. D. L. SMITH, A. P. BURNETT, M. S. BROOKS and D. H. ANTHONY, *J. Dent. Res.* **49** (1970) 283.
3. R. M. GERMAN, *ibid.* **59** (1980) 1960.
4. K. HISATSUNE, K. UDOH, M. NAKAGAWA and K. YASUDA, *Dent. Mater. J.* **6** (1987) 54.
5. K. HISATSUNE, Y. TANAKA, T. TANI, K. UDOH and K. YASUDA, *J. Mater. Sci.: Mater. Med.* **3** (1992) 54.
6. A. KRAWITZ and R. SINCLAIR, *Philos. Mag.* **31** (1975) 697.
7. B. D. CULLITY, in ''Elements of X-ray Diffraction'', 2nd edn (Addison-Wesley Publishing Company, Inc., Reading, MA, 1978) p. 359.
8. B. D. CULLITY, in ''Elements of X-ray Diffraction'', 2nd edn (Addison-Wesley Publishing Company, Inc., Reading, MA, 1978) p. 285.
9. I. R. HARRIS, M. NORMAN and A. W. BRYANT, *J. Less-Common Met.* **16** (1968) 427.

Received 29 November 2000
and accepted 21 September 2001